A Performance Investigation of a Four-Switch Three-Phase Inverter-Fed IM Drives at Low Speeds Using Fuzzy Logic and PI Controllers

Mohamed S. Zaky and Mohamed K. Metwaly

***Abstract*—This paper presents a speed controller using a fuzzy-logic controller (FLC) for indirect field oriented control (IFOC) of induction motor (IM) drives fed by a four-switch three-phase (FSTP) inverter. In the proposed approach, the IM drive system is fed by FSTP inverter instead of the traditional six-switch three-phase (SSTP) inverter for a cost-effective low power applications. The proposed FLC improves dynamic responses and, it is also designed with reduced computation burden. The complete IFOC scheme incorporating the FLC for IM drives fed by the proposed FSTP inverter is built in Matlab/Simulink and, it is also experimentally implemented in real-time using a DSP-DS1103 control board for a prototype 1.1 kW IM. The dynamic performance, robustness, and insensitivity of the proposed FLC with FSTP inverter fed IM drive is examined and compared to a traditional PI controller under speed tracking, load disturbances, and parameters variation, particularly at low speeds. It is found that the proposed FLC is more robust than the PI controller under load disturbances, and parameters variation. Moreover, the proposed FSTP IM drive is comparable with a traditional SSTP IM drive, considering its good dynamic performance, cost reduction and low THD.**

***Index Terms*— FLC; Total Harmonic distortion; FSTP inverter, parameters variation, IFOC.**

I. INTRODUCTION

THREE-PHASE induction motors have been considered one of the most commonly used electric machines in industrial applications due to their low cost, simple and robust construction. Three-phase inverters are considered an essential part in the variable speed AC motor drives. Previously, the traditional six-switch three-phase (SSTP) inverters have been widely used in different industrial applications. These inverters have some drawbacks in low power range applications, which involve extra cost; the six switches losses, and complicated control schemes. Moreover, they require building interface circuits to produce six PWM pulses [1-3]. The development of low-cost motor drive systems is an important topic, particularly for a low-power range. Therefore, the three-phase inverter with reduced component for driving an IM was presented in [1]. Also, reduced switch count has been extended for a rectifier–inverter system with active input current shaping [2]. Three different configurations of IM drives fed from a four-switch inverter to implement low-cost drive systems for low-power range applications have been presented in [3].

Recently, different research works to design new power converters for minimizing losses and costs have been proposed. Four-switch three-phase (FSTP) inverters instead of SSTP inverters have been used in motor drives [4]-[9], renewable energy applications [10], and active power filters [11], [12]. Control of FSTP brushless dc motor drives has been presented in [4]; using DTC with non-sinusoidal back EMF [5], using single current sensor [6] or using DTC with reduced torque ripples [7]. Compensation of inverter voltage drop in DTC for FSTP PM brushless AC drives has been presented in [8]. A DTC strategy for FSTP-inverters with the emulation of the SSTP inverter operation has been presented in [9]. An FSTP inverter has been presented for renewable energy source integration to a generalized unbalanced grid-connected system [10].

Some features of FSTP inverters over the traditional SSTP inverters have been achieved such as minimized switching losses, decreased cost due to reduction in switches number, reduced number of interface circuits, simpler control schemes to produce logic pulses, low computational burden, and more reliability because of lesser interaction between switches [13]-[17]. PWM method of FSTP inverters is improved in [13]. However, it requires more voltage sensors. The problem associated with FSTP inverter is further investigated in [14]. A method to produce PWM pulses to control the FSTP-inverters and compensation of capacitor unbalance has been proposed in [15]. A DC–AC FSTP SEPIC-based inverter has been presented in [16]. This inverter improves the utilization of the dc bus compared to the traditional FSTP inverter. Motor current unbalance of FSTP inverters has been studied with a compensation method utilizing current feedback [17].

The control of IMs is a challenging issue as a result of their nonlinear model and parameters variation. In classical control systems using proportional–integral (PI) and PI–derivative (PID) controllers, the controller performance is significantly reliant on the IM models. However, most of these models are complicated and parameter dependent. Also, they use some assumptions that cause inaccuracy in the mathematical model.

Manuscript received September 28, 2015; accepted June 18, 2016.

M. S. Zaky is with the Department of Electrical Engineering, Faculty of Engineering, Minoufiya University, Shebin El-Kom 32511, Egypt (e-mail: mszaky78@yahoo.com).

M. K. Metwaly is with the Department of Electrical Engineering, Faculty of Engineering, Minoufiya University, Shebin El-Kom 32511, Egypt (e-mail: mohkamel2007@yahoo.com).

Therefore, the model-based controllers, such as a traditional PI and PID controllers, cannot give satisfactory performance under speed tracking changes, load impact, and parameters variation [18]. Several works to design the speed controller of electrical motor drives to overcome the problem of fixed gains PI controllers are recently proposed such as a sliding mode control with disturbance compensation [19], adaptive PID controller [20], model predictive direct control [21], on-line inertia identification algorithm for PI parameters optimization [22], and a data-based PI controller [23].

In recent years, extensive research works have been presented to implement artificial intelligent controllers (AICs) owing to their merits compared to classic PI and PID controllers. The major merits of AICs are that they are independent of the plant mathematical model and their performances are robust under system nonlinearities and uncertainties [18], [24-29]. AICs techniques for SSTP inverters fed IM drive systems include FLC [18, 24], Self-Tuned Neuro-Fuzzy Controller [25-27], Emotional Intelligent Controller [28], and Adaptive Fuzzy Sliding-Mode Control [29]. Also, FLC for IPMSM-based FSTP inverters has been developed in [30].

The rotor flux is essential for an accurate operation of IFOC of IM drives. The field orientation technique needs precise machine parameters to guarantee accurate decoupling of the stator current vector in relation to the rotor flux vector. Using sensors for direct measurement of the rotor flux gives correct value without sensitivity to machine parameters. Nevertheless, this method is problematic, costly and prone to errors in noisy environments. Therefore, flux estimation based on the dynamic model of the IM is highly required for high-performance IFOC of IM drives. A problem is that actual machine parameters vary with operating conditions. Inaccurate machine parameters may cause torque nonlinearity and saturation of the motor. It is possible that the machine control performance degrades due to the parameters mismatch and the system becomes detuned. Consequently, the flux estimation should be as insensitive to varying parameters as possible which is critical to ensure correct field orientation control. The flux estimation with its different techniques is a challenge for both speed-sensored and speed-sensorless drives [31-36].

In the low speed region, the effect of changing the motor parameters (stator and rotor resistances as well as moment of inertia) is especially noticeable on low speed of operation. For speeds lower than 2/3 maximum motor speed, the performance of FSTP inverters is similar to SSTP inverters because the maximum common mode voltage from FSTP is 2/3 of maximum common mode voltage from traditional SSTP inverters [3],[15]. Then, the stable operation of FSTP inverters is till 2/3 of maximum speed. For speeds above 2/3 maximum motor speed, it needs extra DC link voltage for FSTP inverters to achieve IFOC and develop the same performance of the drive system with SSTP inverters.

Previous works have been reported on the application of FLC-based IM drive [18], [24-29]. Also, few works have been presented for the FLC-based IM fed from FSTP inverter. However, these works were restricted to high speed region, and low speed region is not examined [30]. Thus, it is essential to expand FLC-based IM drives during low and high speeds. Also, these works do not provide any results about the effectiveness of FLC under parameters uncertainty in the low speed region. Therefore, there is a strong need for successful development and real-time implementation of the FLC-based IM fed from FSTP inverter, which will be appropriate for cost-effective low power practical applications. Hence, the most important contribution of this paper compared with other works is to investigate the dynamic performance of FSTP inverter fed IM drives using FLC, particularly at low speeds.

This contribution is achieved throughout the following points.

- Investigate the dynamic performance of a FLC-based FSTP inverter fed IM for high-performance industrial applications under speed tracking, load disturbance, and parameters variation, particularly at low speeds.
- Implement the complete IFOC technique of an IM drive fed by the proposed FSTP inverter in Matlab/Simulink, and also, in real-time by a DSP-DS1103 control board for a prototype 1.1 kW IM.
- Verify the robustness of the proposed FLC in comparison to the traditional PI controller using simulation and experimental results at different operating conditions.
- Examine the insensitivity of the two controllers to parameters variation, particularly motor inertia and stator and rotor resistances.
- Compare the performance of the proposed FSTP inverter and the SSTP inverter using total harmonic distortion (THD) of the stator current.

II. Motor Dynamics And Control Scheme

A. Mathematical model of IM and Control Scheme

The representation of the IM in a $d-q$ axis was used, and the control structure relies on the indirect field oriented control (IFOC). Detailed explanation of IFOC model was presented in [37] for non-repetition. The control structure of the proposed FLC-based IFOC of induction motor fed by FSTP voltage source inverter (VSI) is illustrated in Fig. 1. The error between the reference speed, motor speed and the derivative of speed error are the inputs to the FLC and its output is the reference torque T_e^*. The reference currents in *d-q* axis are transformed into the reference motor currents in *a-b-c* axis by inverse Park's transformation. The reference motor currents and their corresponding actual motor currents the differences between these currents are the inputs to hysteresis bands of current controlled VSI to generate pulse width-modulation binary signals, which are utilized to activate the status of FSTP inverter. The motor voltages are produced using FSTP inverter.

B. FSTP Inverter

The power circuit of a FSTP-VSI fed IM is illustrated in Fig. 1. This circuit is composed from two sides. The first side is a half-wave voltage doubler fed from single-phase AC

This article has been accepted for publication in a future issue of this journal, but has not been fully edited. Content may change prior to final publication. Citation information: DOI 10.1109/TPEL.2016.2583660, IEEE Transactions on Power Electronics

power supply. The frequency of the input ac voltage is fixed; this voltage is rectified using rectifier switches Qr1 and Qr2. The rectifier circuit is utilized to charge the capacitor bank in the DC-link. The second side is the FSTP-VSI. The FSTP inverter utilizes four switches: Q1, Q2, Q3, and Q4, respectively, as illustrated in Fig. 1. Phase "*a*" and phase "*b*" of the IM are connected through two limbs of the inverter, while phase "*c*" is connected to the midpoint of the capacitors bank. The FSTP inverter uses four isolated gates bipolar transistors (IGBTs) and four freewheeling diodes to get the two line-to-line voltages V_{ac} and V_{cb}. However, the third line to line voltage (V_{ba}) is obtained using Kirchhoff's voltage law from a split capacitor bank. The maximum dc link voltage across each capacitor maintains equal to V_{dc}. The generated three-phase output voltages using FSTP inverter are balanced with adjustable voltage and frequency. In the current analysis, the FSTP inverter switches are utilized as ideal switches. The three-phase output voltages of the FSTP inverter are obtained using the DC-link voltages V_{dc} and the binary signals of the two limbs of the FSTP inverter. The generated phase voltages fed IM can be expressed as a function of the switching states of the inverter and V_{dc} as follows [30]:

$$\left.\begin{aligned} V_a &= \frac{V_{dc}}{3}(4S_a - 2S_b - 1) \\ V_b &= \frac{V_{dc}}{3}(-2S_a + 4S_b - 1) \\ V_c &= \frac{V_{dc}}{3}(-2S_a - 2S_b + 2) \end{aligned}\right\} \quad (1)$$

where V_{dc} is the peak voltage across the storage capacitors; S_a and S_b are the actual states of the two phases "*a*" and "*b*" represents by two binary logic variables, which determine the conduction state of the inverter. When S_a is 1, switch (Q1) is conducted and switch (Q4), is not, and when S_a is 0, switch (Q4) is conducted and switch (Q1). S_b has the same principle of operation, and V_a, V_b, V_c are motor phase voltages.

For the balanced generated voltages, the four actual combinations of the inverter status are lead to four voltage vectors as shown in Fig. 2. Table I illustrates the possible modes of operation and the generated output voltage vector FSTP inverter as in [30].

Fig. 3 (a) illustrate the simulation study of phase-a current in steady-state and its THD at speed 50 rpm and rated load conditions using a PI controller with FSTP inverter fed IM drive. To provide a fair comparison, the simulation study of steady-state phase-a current and its THD using FLC with the FSTP-inverter-fed IM drive at similar test conditions are illustrated in Fig. 3(b). It is observed that the motor phase-a current in steady-state and its THD of the proposed FLC with FSTP-inverter-fed IM drive has less THD compared with the traditional PI controller. Also, the simulation tests of phase-a current in steady-state and its THD at speed 50 rpm and rated load conditions using the FLC controller with SSTP inverter fed IM drive is illustrated in Fig. 3(c). It is noted that the FLC using FSTP inverter fed IM drive gives less THD compared with the FLC with traditional SSTP inverter-based method.

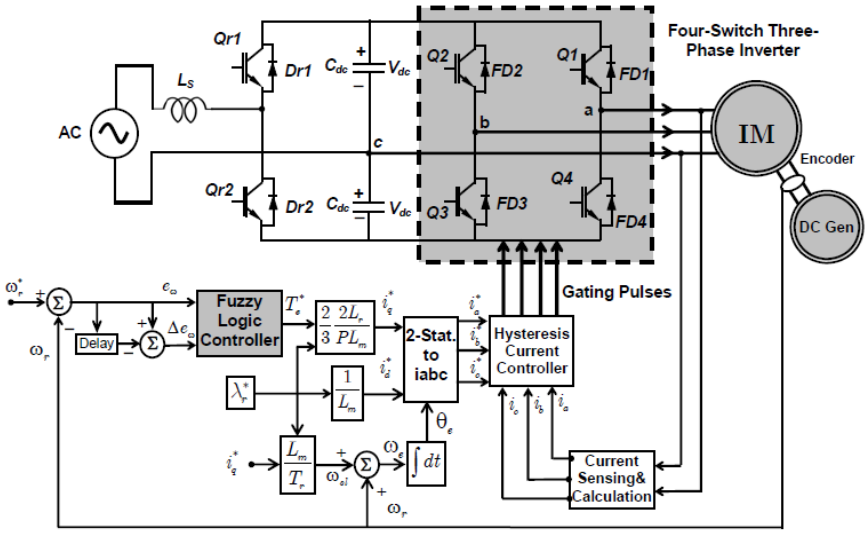

Fig. 1. Block diagram of the proposed FLC-based IFOC scheme of IM drive fed by FSTP voltage source inverter.

This article has been accepted for publication in a future issue of this journal, but has not been fully edited. Content may change prior to final publication. Citation information: DOI 10.1109/TPEL.2016.2583660, IEEE Transactions on Power Electronics

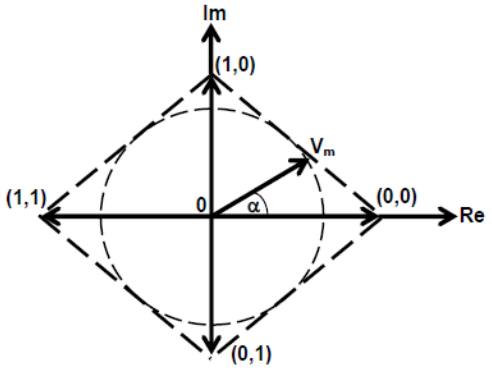

Fig. 2 Switching vectors for a FSTP voltage source inverter.

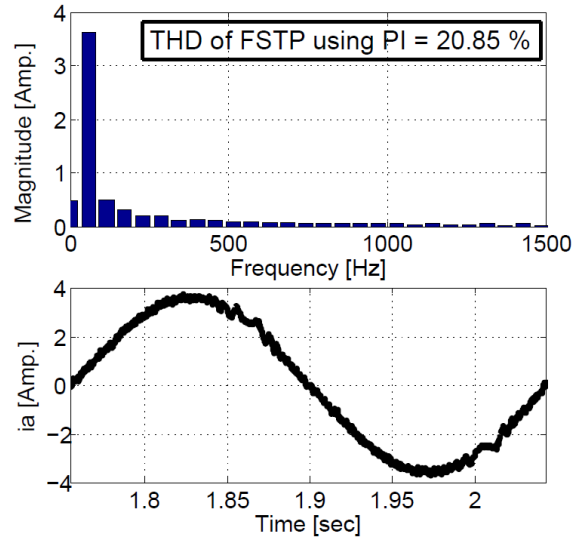

(a)

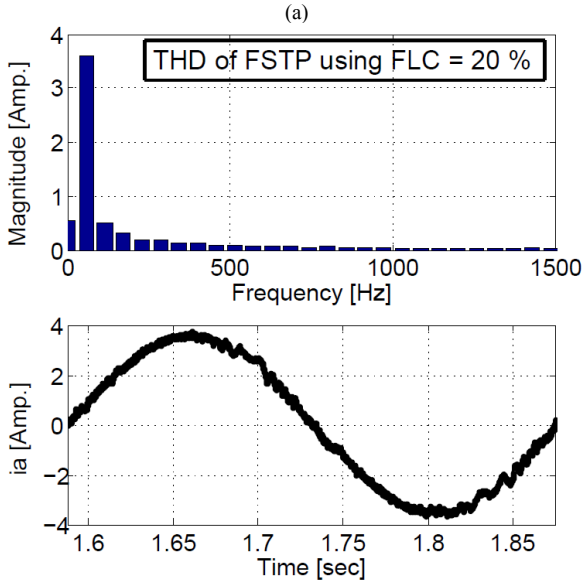

(b)

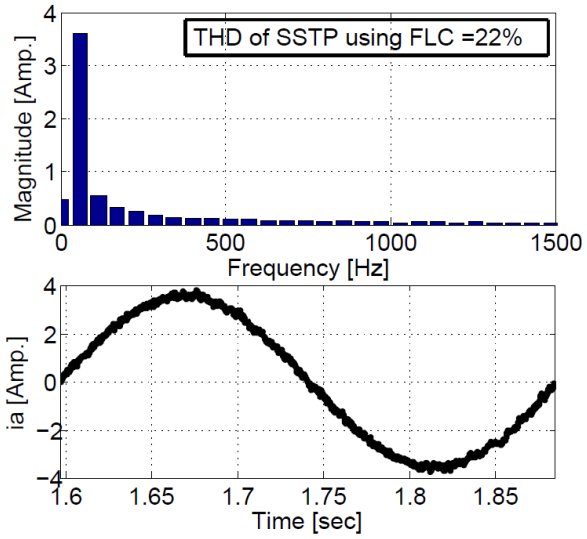

(c)

Fig. 3 Simulation results of steady-state phase current i_a and its harmonic spectrum at speed 50 rpm and rated load conditions using, (a) PI controller-based FSTP inverter fed IM drive, (b) FLC-based FSTP inverter fed IM drive, and (c) FLC-based SSTP inverter fed IM drive.

TABLE I
FSTP INVERTER MODES OF OPERATION

Switching Function		Switch on		Output Voltage Vector		
S_a	S_b			V_a	V_b	V_c
0	0	Q_4	Q_3	$-V_{dc}/3$	$-V_{dc}/3$	$2V_{dc}/3$
0	1	Q_4	Q_2	$-V_{dc}$	V_{dc}	0
1	0	Q_1	Q_3	V_{dc}	$-V_{dc}$	0
1	1	Q_1	Q_2	$V_{dc}/3$	$V_{dc}/3$	$-2V_{dc}/3$

III. Speed Control Methods

A. FLC Algorithm

FLC is used with IM to overcome the problem of developing accurate mathematical description due to load disturbances and parameters changing. The inputs to FLC block are the deviation between the reference and actual motor speeds (speed error) and speed error derivative. These two inputs are utilized to produce the command torque of IM (output of FLC). As illustrated in Fig. 1, the reference torque and reference flux are used to calculate the two reference current components in quadrature and direct axis (i_q^*, i_d^*), respectively. These two currents in combination with the unit vector value are utilized to calculate the three phase reference currents (i_a^*, i_b^*, i_c^*) based on inverse Park's transformation in order to keep the required speed. The main function of FLC is to keep the motor speed aligned with the desired speed, as a result the motor currents kept close to their reference currents. The exact calculations of reference torque depend on the accurate mathematical model of IM as well as its parameters which are really not constant during the motor operation. The effect of motor parameters variations is only noticeable at low speed of operation which is considered as a big challenge for

accurate calculation of the reference torque, as well as exact operation of IM under vector control technique. The intelligent controllers, especially FLC are used with IM drive to overcome the parameters variation at low speed operation. FLC has many features such as, no need for exact mathematical model of IM, and its action depending on linguistic rules with "IF", "AND", and "THEN" operators. This concept is based on human logic. The main drawback of FLC, it needs high calculation burden for simulation and experimental implementations. Therefore, the current paper overcomes this problem by design FLC with low mathematical burden. Many membership functions (MFs) shapes can be chosen based on the designer preference and experience. These MFs are characterized by Gaussian membership. The human perception and experience can be implemented through the MF and fuzzy rules [18].

B. Design of Simplified FLC for IM Drive

The dynamic model of IM expressed as follow;

$$T_e = J\frac{d\omega_r}{dt} + B\omega_r + T_L \quad (2)$$

$$T_e - T_L = J\frac{d\omega_r}{dt} + B\omega_r \quad (3)$$

$$\frac{d\theta_r}{dt} = \omega_r \quad (4)$$

where, J is the rotor inertia, T_e is the electrical torque, T_L is the load torque, B is the frication damping coefficient, and ω_r is the motor speed. Employing small signal model of IM, it can be see that small change of electrical torque ΔT_e resulting in small change of the rotor speed $\Delta\omega_r$. The electrical motor torque equation rewritten as

$$\Delta T_e = J\frac{d\Delta\omega_r}{dt} + B\Delta\omega_r + \Delta T_L \quad (5)$$

The model of small signal in discrete time for the simplified IM model with applying constant load expressed as

$$\Delta T_e(n) = J\Delta e(n) + B\Delta\omega_r(n) + \Delta T_L \quad (6)$$

This equation describing the developed electrical torque as a function of motor speed error and change of error described as follow:

$$T_e(n) = \sum_{n=1}^{N}\Delta T_e(n) = f(\Delta e(n), \Delta\omega_r(n)) \quad (7)$$

where, N is the total number of rules.

$\Delta\omega_r(n) = \omega_r^*(n) - \omega_r(n)$ is the speed error,

$\Delta e(n) = \Delta\omega_r(n) - \Delta\omega_r(n-1)$ is the change of error,

$\Delta\omega_r(n-1)$ is the previous sample of speed error,

$\Delta\omega_r(n)$ is the current value of speed error, $\omega_r(n)$ is the current value of motor speed, and $\omega_r^*(n)$ is the present sample of reference motor speed. A Matlab/Simulink implementation of FLC controller is illustrated in Fig. 4. The FLC algorithm of speed controller employed in the IM drive is based on estimation of two inputs, speed error and its change as illustrated in Fig. 4. These two linguistic variables are considered as input to the system of accordingly interconnected FL block, and the output is the electrical torque command. The derivative block can be replaced by time delay block, which is another way to get the required input. This time delay block would allow shorten the calculation burden, at the same time also secure the controller form uncertainties in the form of spikes in the output, which are the drawback of time derivative block, if the processed signal change abruptly. The time delay block would provide a faster and acceptable robust response and as well as precisely accurate tracking of reference speed. It also allows raising the speed sensor sampling rate significantly.

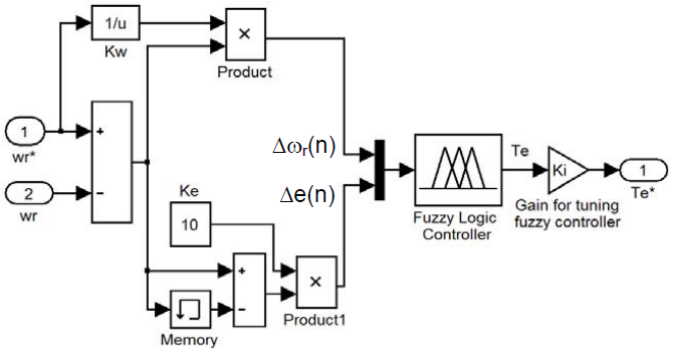

Fig. 4. Block diagram of FLC controller using memory block instead of derivative block.

1) Fuzzification Process

To design the proposed FLC, the first step is to choose the scaling parameters *Kw*, *Ke*, and *Ki* which are determined for fuzzification process and receiving the suitable values of the reference torque. The parameters *Kw* and *Ke* are determined so that the normalized value of speed error and its change, $\Delta\omega_r(n)$ and $\Delta e(n)$ respectively, stays in acceptable limits ± 1. The parameter for the output signal *Ki* is determined so that the rated torque is the output of the FLC at all rated operations. For implementation, the following values are determined $Kw = 1/\omega_r^*$ (command speed), Ke = 10, and Ki = 10 in order to obtain the optimal drive simulations and real time performance. These parameters can be constants or variables and has a significant role for FLC design in order to obtain a good response during all operating conditions [38-39]. In current paper, these parameters are considered constants and are choosed by experimental trial and error to achieve the best possible drive implementation. The MF's of $\Delta\omega_r(n)$, $\Delta e(n)$, and $T_e(n)$ are chosen after selecting scaling parameters. MF's are important elements of the FLC. Figure 5 shows the MFs used for the input and output fuzzy sets of FLC for producing the reference torque. The triangular MF's are utilized for all the fuzzy sets of the input and output vectors because of their ease of mathematical representation. As a result it makes the possible to simplify the implementation of FL inference engine and to reduce the computational burden for real time operation [40].

This article has been accepted for publication in a future issue of this journal, but has not been fully edited. Content may change prior to final publication. Citation information: DOI 10.1109/TPEL.2016.2583660, IEEE Transactions on Power Electronics

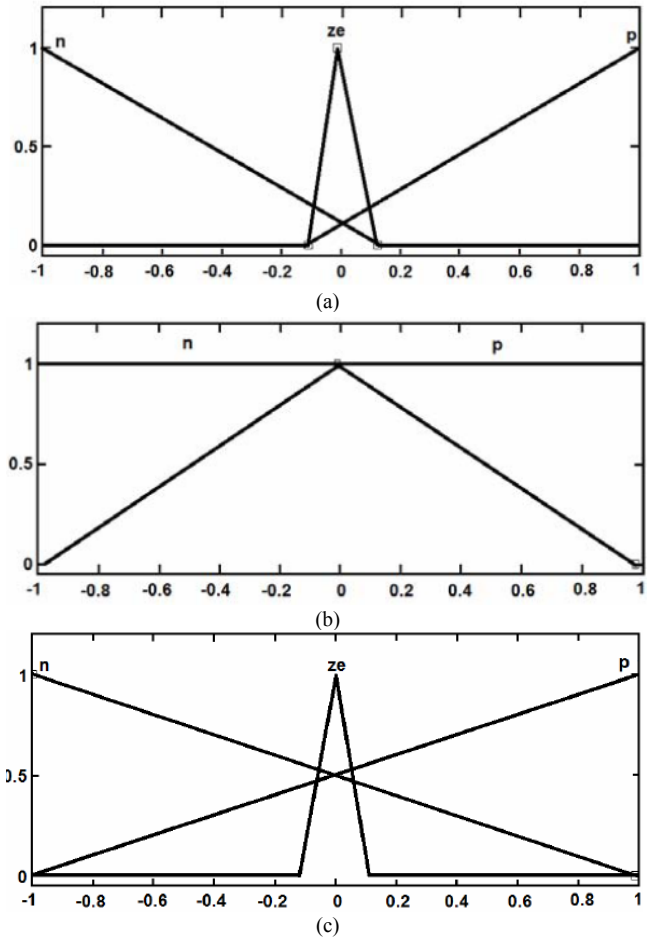

Fig. 5 Membership functions for, (a) speed error $\Delta\omega_r(n)$, (b) change of speed error $\Delta e(n)$, (c) torque reference $T_e(n)$ implemented in Matlab Simulink.

2) Rules Base Process

The margin of universe of discourse of the input vectors $\Delta\omega_r(n)$ and $\Delta e(n)$ and output T_e^* are chosen from -1 to 1. The exact fuzzy rule base of simplified FLC of the input variables to the output is done by fuzzy IF-THEN-AND logic operators rules of six linguistic expressions described in Table II as follows [39]:

TABLE II
RULES BASE PROCESS

1- IF $\Delta\omega_r(n)$ is N (Negative) AND $\Delta e(n)$ is N (Negative) THEN T_e* is ZE (Zero)
2- IF $\Delta\omega_r(n)$ is ZE (Zero) AND $\Delta e(n)$ is N (Negative) THEN T_e* is P (Positive)
3- IF $\Delta\omega_r(n)$ is P (Positive) AND $\Delta e(n)$ is N (Negative) THEN T_e* is P (Positive)
4- IF $\Delta\omega_r(n)$ is N (Negative) AND $\Delta e(n)$ is P (Positive) THEN T_e* is ZE (Zero)
5- IF $\Delta\omega_r(n)$ is ZE (Zero) AND $\Delta e(n)$ is P (Positive) THEN T_e* is ZE (Zero)
6- IF $\Delta\omega_r(n)$ is P (Positive) AND $\Delta e(n)$ is P (Positive) THEN T_e* is P (Positive)

3) Inference and Defuzzification

Fuzzy inference is the complete process of formulating the mapping of the function from given input to an output using fuzzy logic operators. The Mamdani and Sugeno are the two basic types of fuzzy inference methods. The main difference between these types is the way of defining the output. This paper uses the commonly used method for fuzzy inference and defuzzification process which is Mamdani max-min (or sum product) composition with center of gravity method [40]. This method is applied for defuzzification to get $T_e(n)$.

C. Design of the PI controller

Selection of the PI controller parameters will influence the speed response, its settling time, overshoot value and load torque rejection, so they should be adjusted to have optimal response for a fair comparison with the proposed FLC. However, the design of these gains cannot achieve all these characteristics simultaneously as reported in [41-43].

To design the PI controller, the schematic diagram of the speed controller of the IM drive is illustrated in Fig. 6. The open-loop transfer function of Eq. (8) has one zero at $-K_{i\omega}/K_{p\omega}$, and two poles at zero and $-B/J$. The PI controller parameters are designed to have optimal response using root-locus method for pole-zero locations as clarified in Fig. 7. The root-locus plot has been used to select the gains of $K_{i\omega}$ and $K_{p\omega}$ to give the required performance. It is found that the PI gains are $K_{i\omega}=15$ and $K_{p\omega}=8$ to give the best dynamic response.

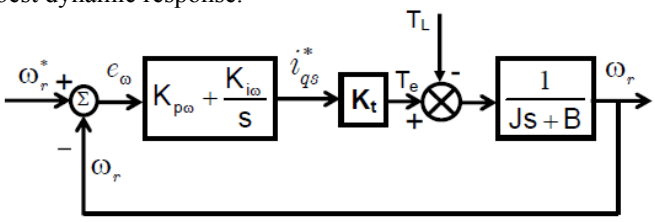

Fig. 6 Block diagram for the speed controller of the IM drive.

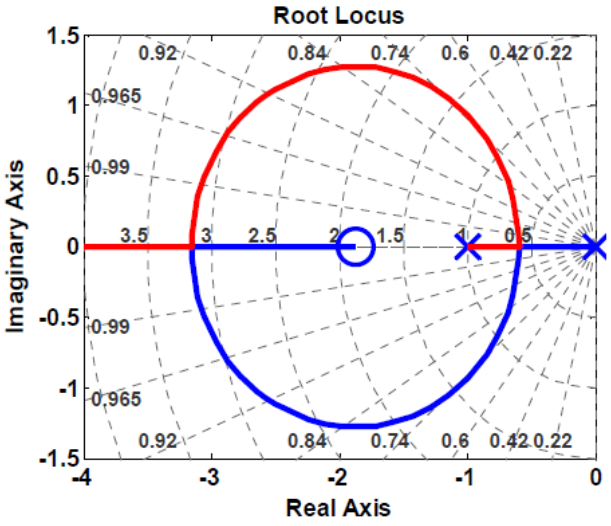

Fig. 7 Root locus plot of the open-loop transfer function with the PI controller gains $K_{p\omega}=8$ and $K_{i\omega}=15$.

$$G_{OL}\big|_{T_L=0} = \frac{K_{p\omega}K_t\left(s + \dfrac{K_{i\omega}}{K_{p\omega}}\right)}{(Js+B)s} \tag{8}$$

IV. Simulation Results

To validate the effectiveness of the fuzzy logic speed controller for the FSTP based-IM drive, a simulation model is built by Matlab/Simulink. The dynamic performance of the proposed IM drive system has been examined using simulation results under various operating conditions. A fair performance comparison between the classical PI controller and the proposed FLC is also provided at identical conditions. The parameters of the IM are given in Table IV.

A. Speed Tracking Performance

Figs. 8(a) and 8(b) demonstrate simulated speed and current signals of the FSTP inverter-fed IM drive using the traditional PI controller and the proposed FLC scheme, respectively, to see the starting performance. The IM drive starts under light load torque and a speed command changed from 0 to 100 rpm. As shown in Fig. 8(b), the IM drive using the FLC tracks the desired speed smoothly without any overshoot, undershoot, and steady-state error, while the traditional PI controller has an overshoot and large rising time to arrive the desired speed as shown in Fig. 8(a). However, according to Fig. 8(a) and Fig 8(b), the stator currents shows an overshoot but it lasts for only 0.033 sec and its value in PI controller is higher than FLC.

Other simulated speed and stator current responses at a sudden speed change are depicted in Figs. 9 and 10 for both the traditional PI controller and FLC. Also, in these cases the FLC-based IM drive ensures the efficacy over the traditional PI controller as the actual speed does not has any overshoot, undershoot, and steady-state error as shown in Figs. 9(b), 10(b) when compared with the same figures (9(a), 10(a)) using the traditional PI controller. Thus, the FLC-based IM drive fed from FSTP inverter proves a good performance under speed reference tracking.

B. Load Torque Disturbance

The robustness of a FSTP inverter fed IM drive for both the traditional PI controller and FLC is also examined for sudden load change at a speed reference 20 rpm as shown in Fig. 11. At *t = 2 sec*, a rated torque of 7 N.m is applied. It is found that the FLC-based IM drive system confirms the effectiveness over the traditional PI controller as the actual speed has a low speed dip and recovers quickly with minimum time during sudden load torque, whereas the stator current rapidly arrives to the new equivalent value of the rated torque. Therefore, good speed tracking performance and good load torque rejection is attained using FLC-based IM drive, while, the PI-controller-based IM drive incapable of achieving the desired performance sudden change in reference speed and torque disturbance.

C. Effect of Parameters Variation

The two speed controllers are examined at low speeds under parameters variation. Figs. 12(a) and 12(b) show the simulated responses of speed, stator currents, and a quadrature current of a FSTP inverter fed IM drive for a sudden increase in stator and rotor resistances at a speed reference 20 rpm using the traditional PI controller and FLC. The mismatch of 100% in the stator and rotor resistance values is tested to prove the robustness of the FLC. The first graph of Fig. 12(b) shows the simulated reference and actual speeds. It is observed that the actual speed tracks the reference speed in spite of stator and rotor resistance mismatches using the proposed FLC controller. The next graph shows the stator current. It is clear that the frequency of stator current is changed due to the increase of the slip speed from time t = 1.5 sec due to the effect of changing the rotor and stator resistances. The third graph shows the q-component current i_q^*. It is found that the current i_q^* show insignificant changes at time t = 1.5 sec for the mismatches in the rotor and stator resistances. The fourth graph demonstrates the mismatch of 100% in the stator and rotor resistances values that are introduced in the simulation model of the IM at time t = 1.5 sec. It is evident that in the first graph that the proposed FLC controller is robust under parameter mismatches and the speed tracking is not affected. However, the first graph of Fig. 12(a) exhibits small variation in the speed under the variation of stator and rotor resistances

Other simulated responses under inertia variation are also presented to examine the robustness of the two speed controllers. The IM drive is tested with inertia ($J = 1.5J_o$). Fig. 13(a) illustrates simulated speed and trajectory tracking responses of a FSTP inverter fed IM drive under motor inertia variations for a speed reference of 20 rpm using the traditional PI controller. The same figure at identical conditions is depicted using the proposed FLC for performance comparison purposes as seen in Fig. 13(b). Fig. 13 justifies the robustness of the proposed FLC in comparison to the traditional PI controller. As clear, traditional PI controller has a substantial variation in the speed response at J = 1.5 Jo. However, the proposed FLC remains insensitive under the identical inertia variation. The phase plane trajectory of the second graph in Figs. 13(a) and 13(b), validates this superiority of the proposed controller.

This article has been accepted for publication in a future issue of this journal, but has not been fully edited. Content may change prior to final publication. Citation information: DOI 10.1109/TPEL.2016.2583660, IEEE Transactions on Power Electronics

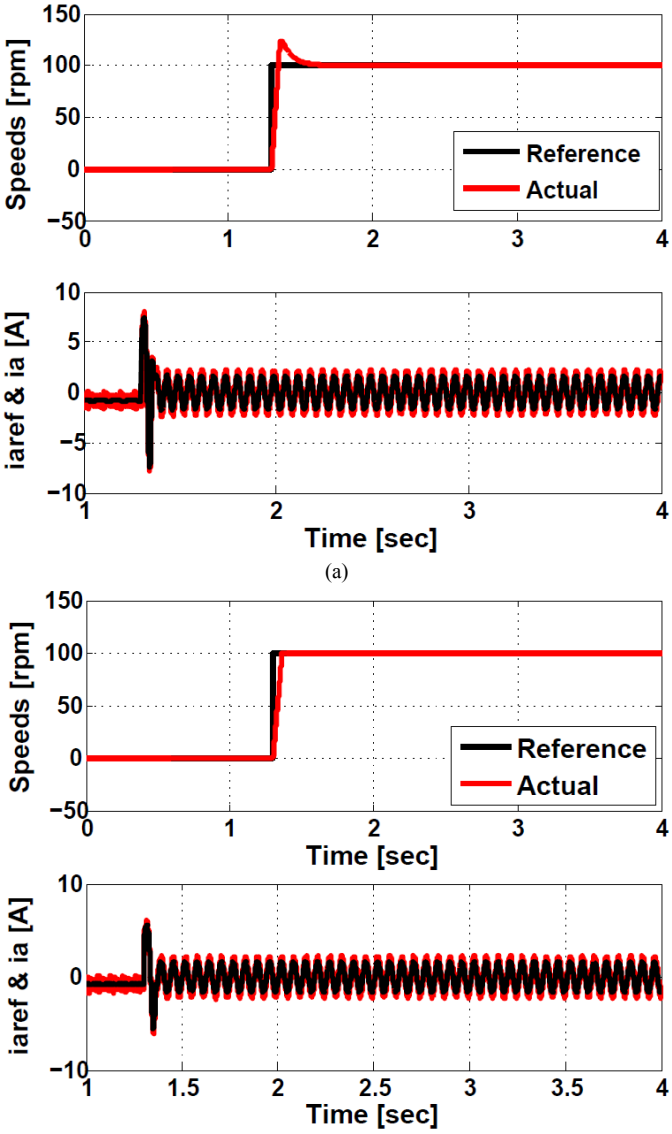

Fig. 8 Simulated speed and stator currents responses of a FSTP inverter fed IM drive for a starting operation at low speed with a step change of a speed reference from 0 to 100 rpm using, (a) Traditional PI controller, and (b) Proposed FLC.

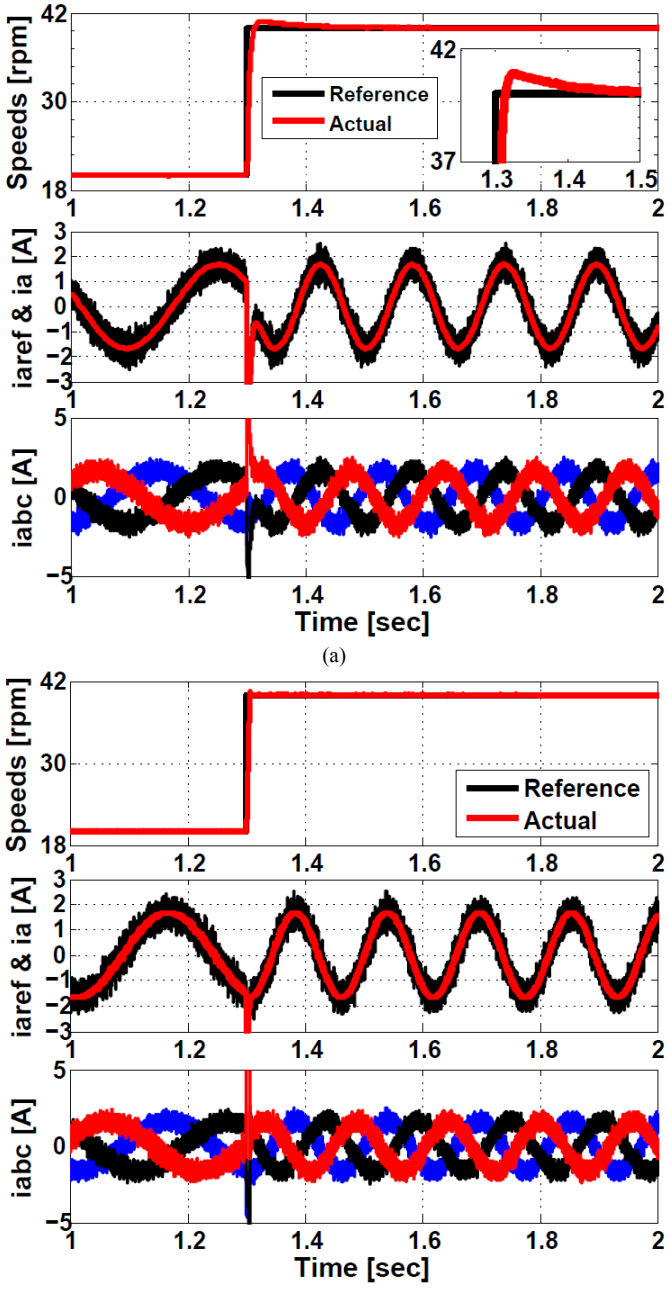

Fig. 9 Simulated speed and stator currents responses of a FSTP inverter fed IM drive for a step change of a speed reference from 20 to 40 rpm using, (a) Traditional PI controller, and (b) Proposed FLC.

This article has been accepted for publication in a future issue of this journal, but has not been fully edited. Content may change prior to final publication. Citation information: DOI 10.1109/TPEL.2016.2583660, IEEE Transactions on Power Electronics

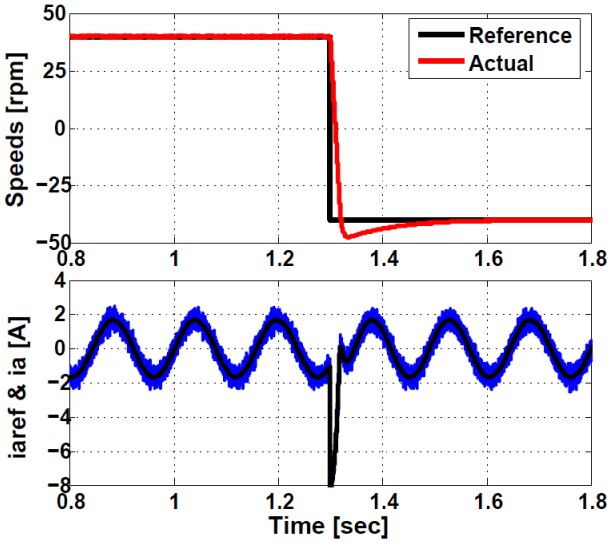

(a)

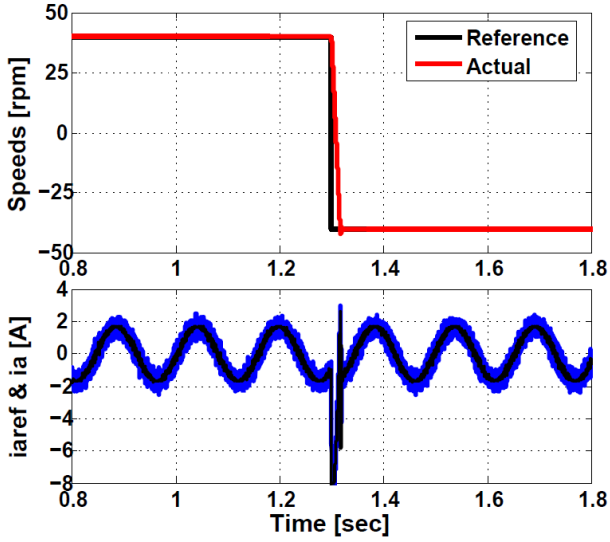

(b)

Fig. 10 Simulated speed and stator currents responses of a FSTP inverter fed IM drive for a speed reversal from 40 to –40 rpm using, (a) Traditional PI controller, and (b) Proposed FLC.

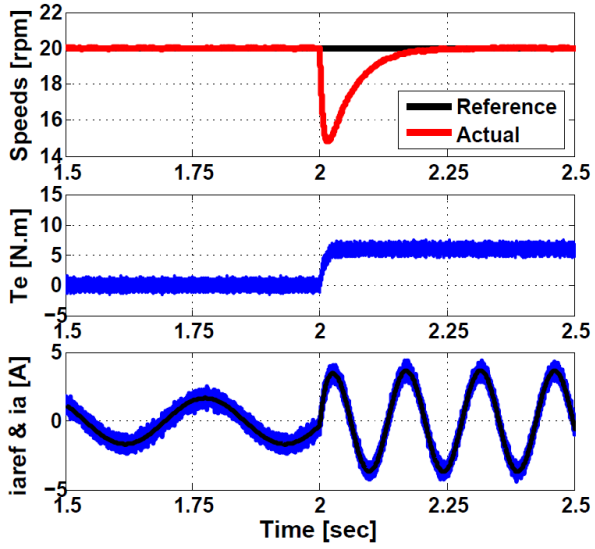

(a)

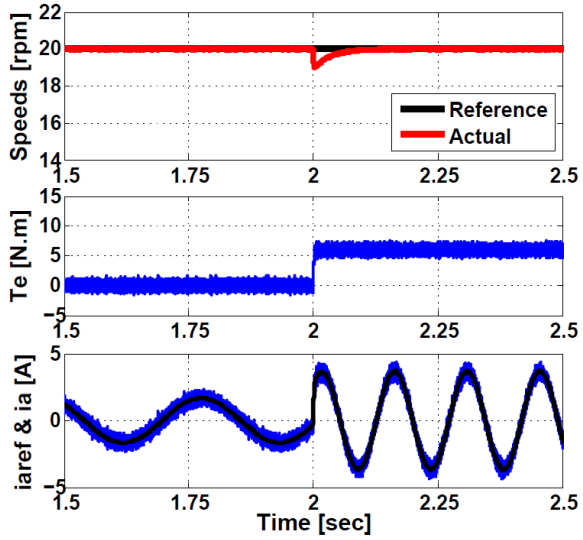

(b)

Fig. 11 Simulated speed and stator currents responses of a FSTP inverter fed IM drive for a sudden increase in load of 7 N.m at a speed reference 20 rpm using, (a) Traditional PI controller, and (b) Proposed FLC.

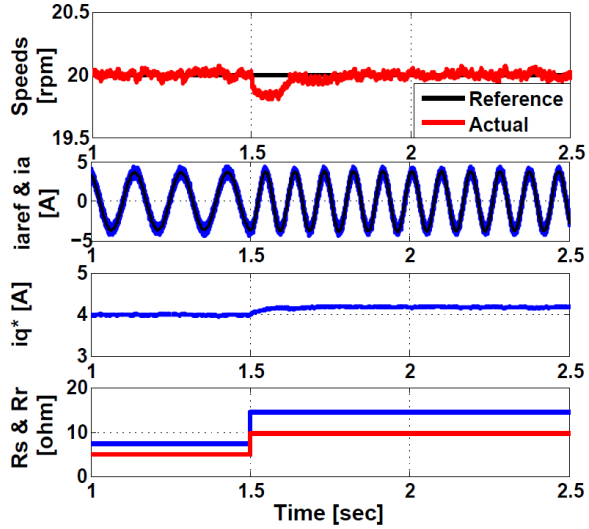

(a)

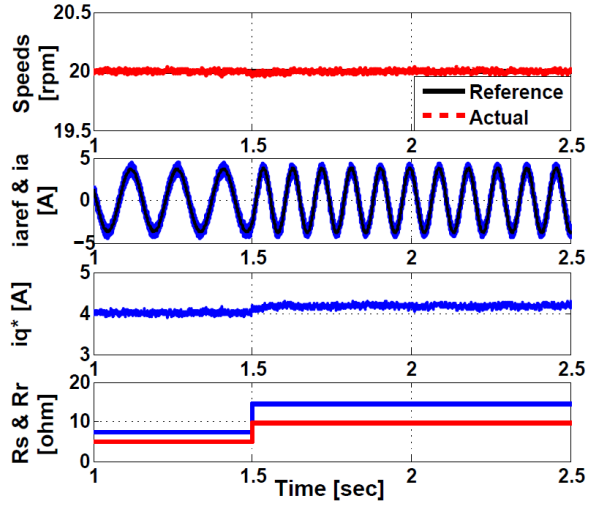

(b)

Fig. 12 Simulated speed, stator currents, and quadrature current responses of a FSTP inverter fed IM drive for a sudden increase in stator and rotor resistances at a speed reference 20 rpm using, (a) Traditional PI controller, and (b) Proposed FLC.

This article has been accepted for publication in a future issue of this journal, but has not been fully edited. Content may change prior to final publication. Citation information: DOI 10.1109/TPEL.2016.2583660, IEEE Transactions on Power Electronics

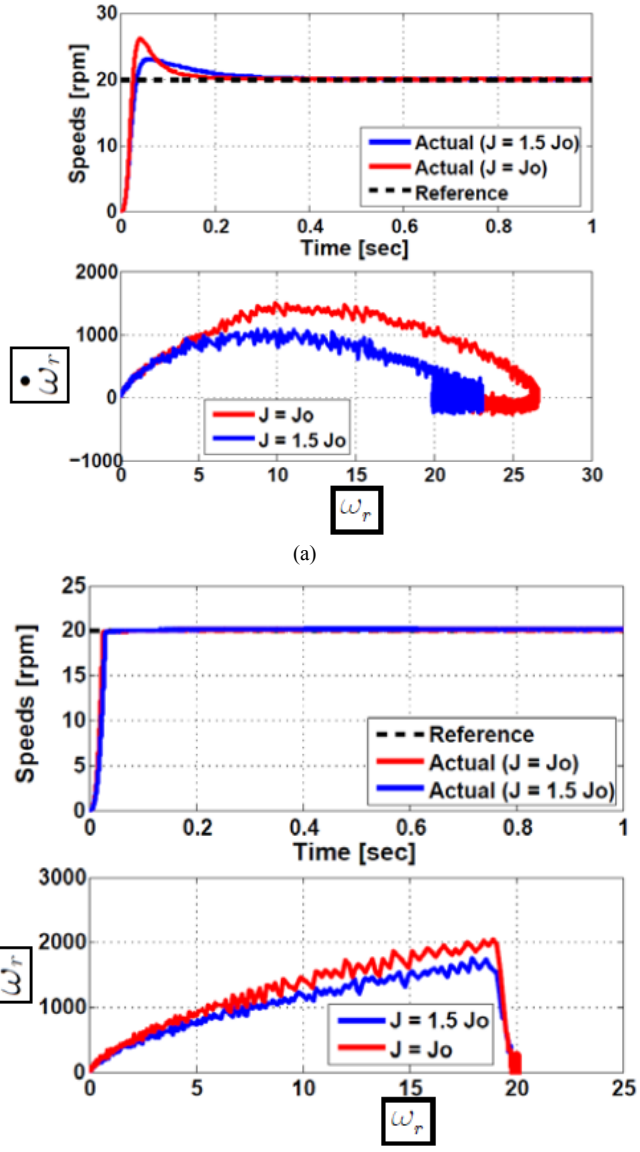

Fig. 13 Simulated speed and trajectory tracking responses of a FSTP inverter fed IM drive under motor inertia variations for a speed reference of 20 rpm using, (a) Traditional PI controller, and (b) Proposed FLC.

V. Experimental Setup and Results

A. Drive system setup

The behaviors of proposed FLC-based IM control have been evaluated using Simulink benchmark and then verified by experimental implementation in real-time using digital signal processing (DSP-DS1103) control card for a laboratory 1.1 kW IM as illustrated in Fig. 14. The parameters of the used IM are listed in Table IV in the appendix. The IM is supplied by FSTP-VSI using four IGBT's and a gate driver board. The control is done using DSP-DS1103 control board which is interfaced with personal computer (PC) through the control panel. The control panel contains a lot of peripherals such as digital-to-analog (D/A), analog-to-digital (A/D) converters and position encoder interfaces. It also provides the required digital input output I/O ports and timer function such as input, output captures, and generation of inverter pulses. All computations are done and programmed on Simulink benchmark through a PC. The real-time Simulink model is built and downloaded to Matlab environment through the DSP-DS1103 control board.

The inverse Park's transformations are used to obtain the three-phase reference motor current from the reference direct and quadrature axis currents. The motor currents are measured using the current transducers as inputs to the DSP control board. The hysteresis current controller utilizes the difference between the actual motor currents and the corresponding reference motor currents to produce the four PWM pulses to operate the FSTP inverter. The output voltages from FSTP inverter are utilized to supply the IM with suitable voltages and frequency corresponding to the operating condition. An incremental encoder with 1024-pulse resolution is used to sense the rotor position and speed this encoder is interfaced with DSP-DS1103 through the control panel terminal. The IM is connected to a dc generator for mechanical loading. Fig. 15 shows a laboratory picture of an IM drive system.

B. Experimental Results

Sample of the experimental verifications are illustrated to verify the simulation results as well as to prove the efficiency of the proposed FLC compared with traditional PI controller, particularly at low speeds.

1) Step Speed Reference Change

Fig. 16(a) and (b) demonstrate motor speed and stator currents behavior of a FSTP inverter fed IM drive for a starting operation at low speed with speed reference change from 0 to 100 rpm in step using the traditional PI controller as well as the proposed FLC. This figure is presented in comparison to the simulation results of Fig. 8. Another experimental result for the same variables is presented during the speed reference change from 20 to 40 rpm in step as illustrated in Fig. 17. The experimental figures show that the FLC-based FSTP inverter fed IM drive system has a good performance compared with the PI-based system. These results also illustrate that transient response due to sudden change in reference speed can be handled fast without problems using the proposed FLC; whereas the PI-controller has an overshoot and the transient response is not fast compared to the FLC.

2) Speed Reversal

The two controllers are also tested experimentally under speed reversal from 20 to –20 rpm as given in Fig. 18. This figure prove that the simplified FLC has a good speed tracking behavior during speed reversal compared to the PI controller, which has overshoot and undershoot.

3) Sudden Load Impact

The robustness of the proposed FLC is examined under sudden load change from light load to full-load (7 N.m) when reference speed equal to 20 rpm as illustrated in Fig. 19(b). The same result is taken with the PI controller as shown in Fig. 19(a). The superiority of the FLC is proved compared to the traditional PI controller. Since FLC achieves small speed dip and fast recovery time to its reference speed.

This article has been accepted for publication in a future issue of this journal, but has not been fully edited. Content may change prior to final publication. Citation information: DOI 10.1109/TPEL.2016.2583660, IEEE Transactions on Power Electronics

4) Parameters Variation

The performance of the two controllers under parameters variation is tested using inertia variation as seen in Fig. 20(a) and 20(b) for both controllers. The results ensure that the FLC gives good performance compared to the PI controller.

Table III shows a performance comparison between the FLC and PI controllers using the simulation and experimental results. This comparison includes the speed response, stator current, and the torque disturbance. The performance of the two controllers is comparable in some cases. However, the FLC shows a good behavior than the PI controller.

The speed tracking capability of the FLC is investigated at low speed operation. Thus, the proposed FLC-based drive proves its superiority to the traditional PI-controller-based system under speed tracking, load disturbance, and parameters variation and, hence, FLC is an accurate and robust controller for high-performance low power, and low cost industrial applications.

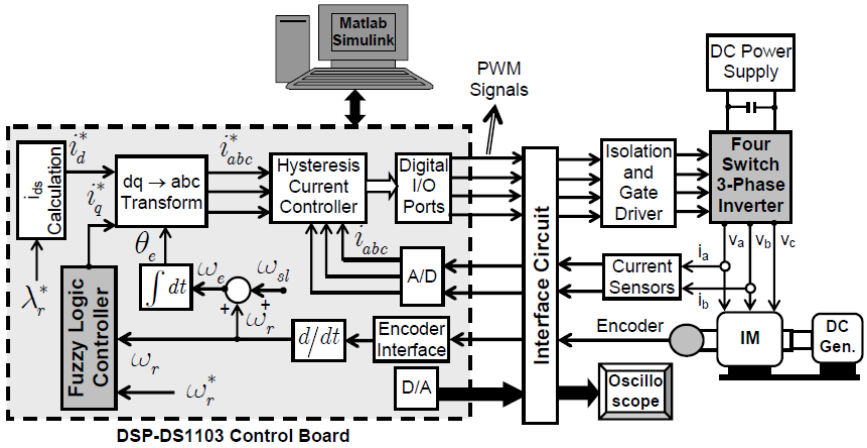

Fig. 14 Schematic diagram of the experimental system for FLC based IFOC of an IM drive fed by FSTP inverter using DSP-DS1103 control board.

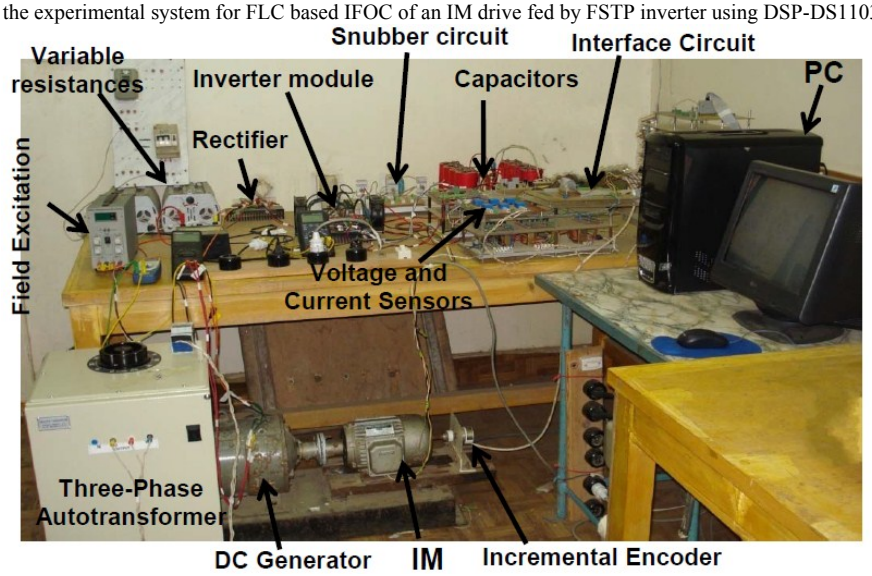

Fig. 15 A laboratory picture of an IM drive system using DSP-DS1103 control board.

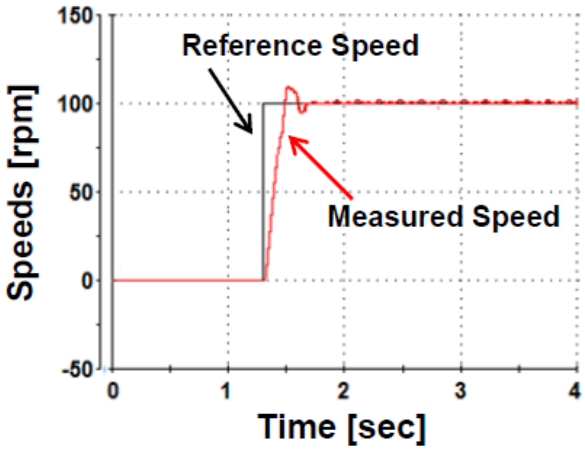

(a)

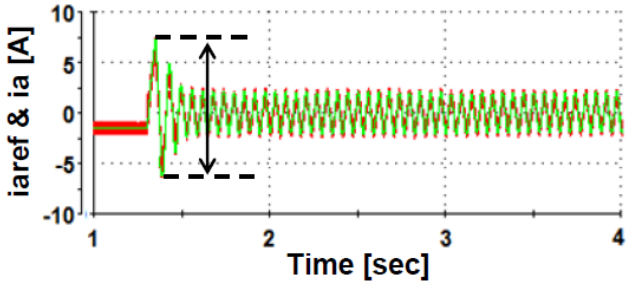

(b)

This article has been accepted for publication in a future issue of this journal, but has not been fully edited. Content may change prior to final publication. Citation information: DOI 10.1109/TPEL.2016.2583660, IEEE Transactions on Power Electronics

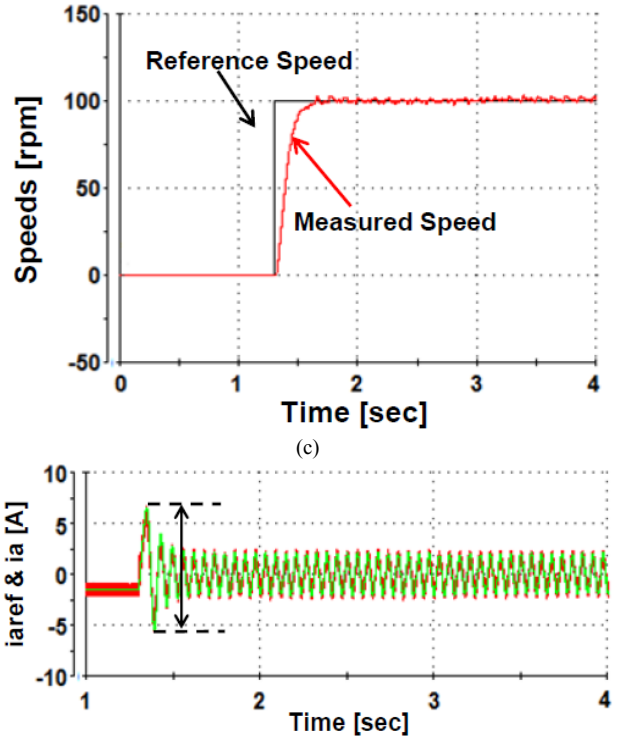

Fig. 16 Experimental speed and stator currents responses of a FSTP inverter fed IM drive for a starting operation at low speed with a step change of a speed reference from 0 to 100 rpm using, (a,b) Traditional PI controller, and (c,d) Proposed FLC.

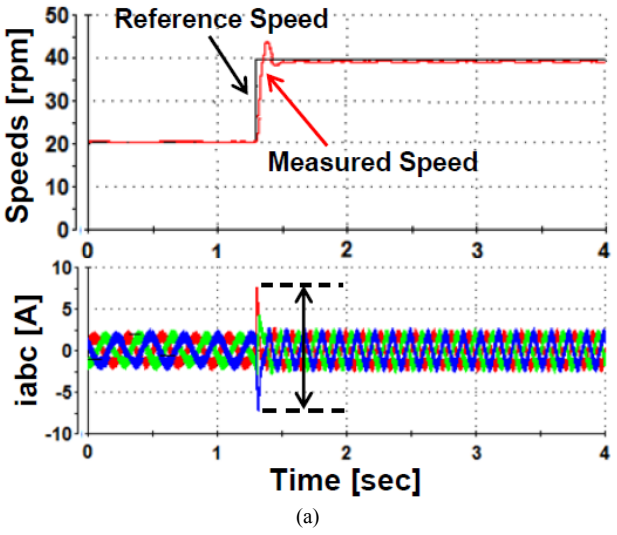

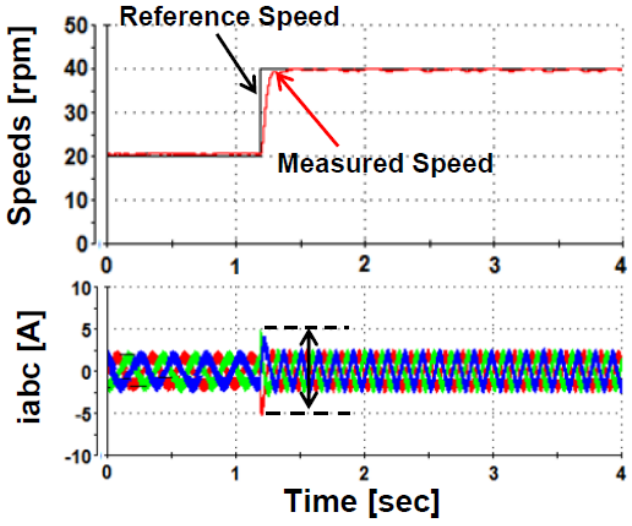

Fig. 17 Experimental speed and stator currents responses of a FSTP inverter fed IM drive a step change of speed reference from 20 to 40 rpm using, (a) Traditional PI controller, and (b) Proposed FLC.

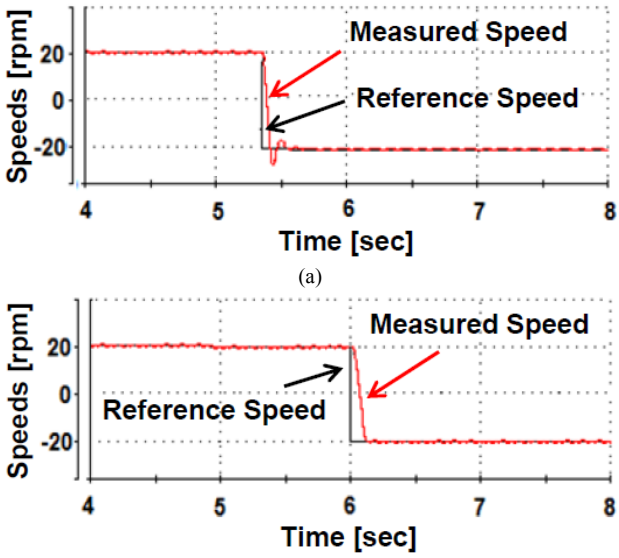

Fig. 18 Experimental speed responses of a FSTP inverter fed IM drive under motor speed reverse at a speed reference from 20 rpm to –20 rpm using, (a) Traditional PI controller, and (b) Proposed FLC.

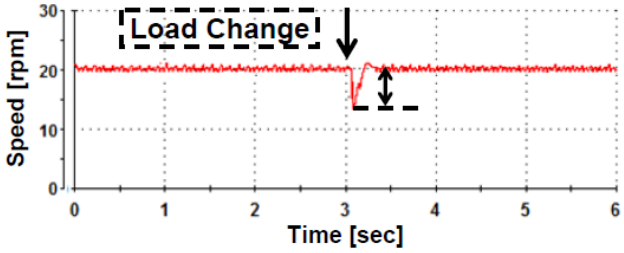

This article has been accepted for publication in a future issue of this journal, but has not been fully edited. Content may change prior to final publication. Citation information: DOI 10.1109/TPEL.2016.2583660, IEEE Transactions on Power Electronics

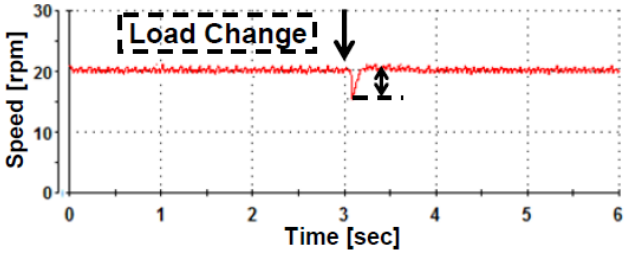

(b)

Fig. 19 Experimental speed responses of a FSTP inverter fed IM drive under a sudden load change at a speed reference from 20 rpm using, (a) Traditional PI controller, and (b) Proposed FLC.

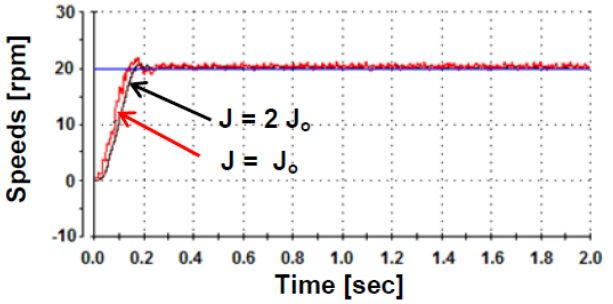

(a)

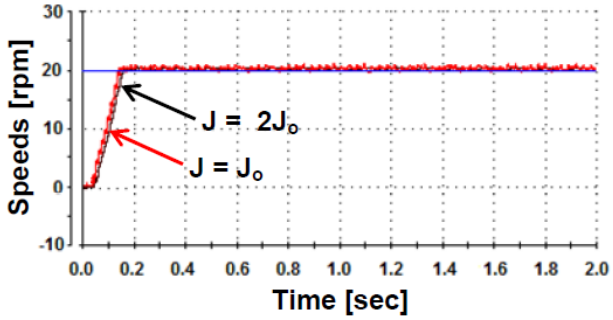

(b)

Fig. 20 Experimental speed responses of a FSTP inverter fed IM drive motor under inertia mismatch at a speed reference of 20 rpm using, (a) Traditional PI controller, and (b) Fuzzy Logic Controller.

TABLE III
PERFORMANCE COMPARISON OF FLC AND PI CONTROLLER

IM Response		Simulation Results		Experimental Results	
		FLC	PI Controller	FLC	PI Controller
Speed Response	Rise Time	50 msec	50 msec	200 msec	200 msec
	Overshoot	0 rpm	20 rpm	1 rpm	12 rpm
	Settling Time	50 msec	300 msec	300 msec	320 msec
Stator Current	Starting	6 Amp.	8 Amp.	6.5 Amp	8 Amp.
	Overshoot %	300 %	400%	325 %	400%
Torque	Speed dip	1 rpm	5 rpm	4 rpm	6rpm
	Recovery time	150 msec	300 msec	250 msec	400 msec

VI. Conclusion

The proposed FLC-based IFOC for an IM drive fed by FSTP inverter has been effectively implemented practically by the DSP-DS1103 control board for a laboratory 1.1 kW IM, and by a computer simulation. The dynamic speed response of the IM drive at low speeds is improved using the FLC which is designed with low computation burden to be appropriate for real-time applications. The validity of the proposed FLC has been examined both in simulation and experimentation at various speed reference tracking and load torque disturbances, particularly at low speeds. To confirm the efficacy of the proposed controller, a fair performance comparison of the proposed FLC-based IM drive with a PI controller has been presented. The robustness of the two controllers has been also examined under parameters variation, especially motor inertia, and stator and rotor resistances. Comparative simulation and experimental results demonstrate that the proposed FLC of a FSTP inverter fed IM drive is superior to the PI controller under speed tracking, load disturbances, and parameters variation. The usefulness of the FLC has been verified by its high dynamic speed response without overshoot and undershoot, and with zero steady-state error, and less THD of stator currents. This shows the good capability of FLC controller during speed tracking performance, disturbance rejection, and parameters variation. The proposed IM drive system is also suitable for cost-effective low power industrial applications.

Appendix

TABLE IV
PARAMETERS OF IM

Rated power	1.1 kW	Stator leakage inductance	0.0221 H
Rated current	2.545 Amp	Mutual inductance	0.4114 H
No. of poles	4	Supply frequency	50 Hz
Stator resistance	7.4826 ohm	Supply voltage	380 volts
Rotor resistance	3.6840 ohm	Inertia	0.02 kg.m^2
Rotor leakage inductance	0.0221 H	Rated voltage	380 V

References

[1] H. W. van der Broeck and J. D. van Wyk, "A comparative investigation of three-phase induction machine drive with a component minimized voltage-fed inverter under different control options," IEEE Trans. Ind. Applicat., vol. 20, pp. 309–320, Mar./Apr. 1984.

[2] P. Enjeti and A. Rahman, "A new single-phase to three-phase converter with active input current shaping for low cost ac motor drives," IEEE Transactions on Industry Applications, Vol. 29, No. 4, pp. 806-813, July/August 1993.

[3] C. B. Jacobina, M. B. R. Correa, E. R. C da Silva, and A. M. N. Lima, "Induction motor drive system for low power applications," IEEE Transactions on Industry Applications, Vol. 35, No. 1, Pp. 52-61, January/February 1999.

[4] C.-T. Lin, C.-W. Hung, and C.-W. Liu, "Position sensorless control for four-switch three-phase brushless DC motor drives," IEEE Trans. on Power Electron., vol. 23, no. 1, pp. 438–444, Jan. 2008.

[5] S. B. Ozturk, W. C. Alexander, and H. A. Toliyat, "Direct torque control of four-switch brushless DC motor with non-sinusoidal back EMF," IEEE Trans. on Power Electron., vol. 25, no. 2, pp. 263–271, Feb. 2010.

[6] C. Xia, Z. Li, and T. Shi, "A control strategy for four-switch three-phase brushless DC motor using single current sensor," IEEE Trans. on Ind. Electron., vol. 56, no. 6, pp. 2058–2066, Jun. 2009.

[7] M. Masmoudi, B. El Badsi, and A. Masmoudi, "DTC of B4-Inverter-Fed BLDC motor drives with reduced torque ripple during sector-to sector commutations," IEEE Trans. on Power Electron., vol. 29, no. 9, pp. 4855–4865, Sep. 2014.

[8] K. D. Hoang, Z. Q. Zhu, and M. P. Foster, "Influence and compensation of inverter voltage drop in direct torque-controlled four-switch three-phase PM brushless AC drives," IEEE Trans. on Power Electron., vol. 26, no. 8, pp. 2343–2357, Aug. 2011.

[9] El Badsi, B., Bouzidi, B., and Masmoudi, A., "DTC scheme for a four-switch inverter-fed induction motor emulating the six-switch inverter operation," IEEE Trans. on Power Electron., Vol. 28, No. 7, pp. 3528–3538, July 2013.

[10] S. Dasgupta, S. N. Mohan, S. K. Sahoo, and S. K. Panda, "Application of four-switch-based three-phase grid-connected inverter to connect renewable energy source to a generalized unbalanced microgrid system," IEEE Trans. on Ind. Electron., vol. 60, no. 3, pp. 1204–1215, Mar. 2013.

[11] W.Wang, A. Luo, X. Xu, L. Fang, T. Minh Chau, and Z. Li, "Space vector pulse-width modulation algorithm and DC-side voltage control strategy of three-phase four-switch active power filters," IET Power Electron., vol. 6, no. 1, pp. 125–135, Jan. 2013.

[12] X. Tan, Q. Li, H. Wang, L. Cao, and S. Han, "Variable parameter pulse width modulation-based current tracking technology applied to four switch three-phase shunt active power filter," IET Power Electron., vol. 6, no. 3, pp. 543–553, Mar. 2013.

[13] F. Blaabjerg, D. O. Neacsu, and J. K. Pedersen, "Adaptive SVM to compensate dc-link voltage ripple for four-switch, three-phase voltage source inverter," IEEE Trans. on Power Electron., vol. 14, no. 4, pp. 743–751, Jul. 1999.

[14] R. Wang, J. Zhao, and Y. Liu, "A comprehensive investigation of four switch three-phase voltage source inverter based on double Fourier integral analysis," IEEE Trans. on Power Electron., vol. 26, no. 10, pp. 2774–2787, Oct. 2011.

[15] Correa, M. B. R., Jacobina, C. B., Da Silva, E. R. C., and Lima, A. M. N., "A general PWM strategy for four-switch three phase inverters," IEEE Trans. on Power Electron., Vol. 21, No. 6, pp. 1618–1627, November 2006.

[16] Mohamed S. Diab, Ahmed Elserougi, Ahmed M. Massoud, Ayman S. Abdel-Khalik, and Shehab Ahmed, "A Four-Switch Three-Phase SEPIC-Based Inverter," IEEE Transactions on Power Electronics, Vol. 30, No. 9, pp.4891-4905, September 2015.

[17] J. Kim, J. Hong, and K. Nam, "A current distortion compensation scheme for four-switch inverters," IEEE Trans. on Power Electron., vol. 24, no. 4, pp. 1032–1040, Apr. 2009.

[18] M. N. Uddin, T. S. Radwan, and M. A. Rahman, "Performances of fuzzy logic based indirect vector control for induction motor drive," IEEE Trans. on Ind. Appl., vol. 38, no. 5, pp. 1219–1225, Sep./Oct. 2002.

[19] Zhang, X.; Sun, L.; Zhao, K.; Sun, L.; , "Nonlinear Speed Control for PMSM System Using Sliding-Mode Control and Disturbance Compensation Techniques," IEEE Transactions on Power Electronics, vol.28, no.3, pp.1358-1365, March 2013.

[20] Jung, J.-W.; Leu, V.Q.; Do, T.D.; Kim, E.-K.; Choi, H.H.; "Adaptive PID Speed Control Design for Permanent Magnet Synchronous Motor Drives," IEEE Transactions on Power Electronics, vol.30, no.2, pp. 900-908, Feb. 2015.

[21] Preindl, M.; Bolognani, S.; , "Model Predictive Direct Speed Control with Finite Control Set of PMSM Drive Systems," IEEE Transactions on Power Electronics, vol. 28, no. 2, pp. 1007-1015, Feb. 2013.

[22] Niu, L.; Xu, D.; Yang, M.; Gui, X.; Liu, Z.; "On-line Inertia Identification Algorithm for PI Parameters Optimization in Speed Loop," IEEE Transactions on Power Electronics, vol.30, no.2, pp. 849-859, Feb. 2015.

[23] Fnaiech, M.A.; Khadraoui, S.; Nounou, H.N.; Nounou, M.N. ;Guzinski, J.; Abu-Rub, H.; Datta, A.; Bhattacharyya, S.P."A Measurement Based Approach for Speed Control of Induction Machines", IEEE Journal of Emerging and Selected Topics in Power Electronics, vol.2, no.2, pp. 308-318, Jun. 2014.

[24] Mavungu Masiala, Behzad Vafakhah, John Salmon, and Andrew M. Knight, "Fuzzy Self-Tuning Speed Control of an Indirect Field-Oriented Control Induction Motor Drive," IEEE Transactions on Industry Applications, Vol. 44, No. 6, Pp.1732-1739, November/December 2008.

[25] M. Nasir Uddin, and Hao Wen, "Development of a Self-Tuned Neuro-Fuzzy Controller for Induction Motor Drives," IEEE Transactions on Industry Applications, Vol. 43, No. 4, Pp. 1108-1116, July/August 2007.

[26] M. Nasir Uddin, Zhi Rui Huang, and A. B. M. Siddique Hossain, "Development and Implementation of a Simplified Self-Tuned Neuro–Fuzzy-Based IM Drive, " IEEE Transactions on Industry Applications, Vol. 50, No. 1, pp. 51-59, January/February 2014.

[27] M. Hafeez, M. Nasir Uddin, Nasrudin Abd. Rahim, and Hew Wooi Ping, "Self-Tuned NFC and Adaptive Torque Hysteresis-Based DTC Scheme for IM Drive, " IEEE Transactions On Industry Applications, Vol. 50, No. 2, Pp. 1410-1419, March/April 2014.

[28] G. R. Arab Markadeh, Ehsan Daryabeigi, Caro Lucas, and M. Azizur Rahman, "Speed and Flux Control of Induction Motors Using Emotional Intelligent Controller," IEEE Transactions on Industry Applications, Vol. 47, No. 3, pp.1126-1135, May/June 2011.

[29] Ali Saghafinia, Hew Wooi Ping, Mohammad Nasir Uddin, and Khalaf Salloum Gaeid, "Adaptive Fuzzy Sliding-Mode Control Into Chattering-Free IM Drive," IEEE Transactions On Industry Applications, Vol. 51, No. 1, pp. 692-701, January/February 2015.

[30] M. Nasir Uddin, Tawfik S. Radwan, and M. Azizur Rahman, "Fuzzy-Logic-Controller-Based Cost-Effective Four-Switch Three-Phase Inverter-Fed IPM Synchronous Motor Drive System," IEEE Transactions on Industry Applications, Vol. 42, No. 1, pp. 21-30, January/February 2006.

[31] Habib-ur Rehman," Elimination of the Stator Resistance Sensitivity and Voltage Sensor Requirement Problems for DFO Control of an Induction Machine," IEEE Transactions on Industrial Electronics, vol. 52, no. 1, pp. 263-269, February 2005.

[32] R. Krishnan and F. C. Doran, "Study of parameter sensitivity in high performance inverter-fed induction motor drive systems," IEEE Trans. Ind. Applicat., vol. IA-23, pp. 623–635, July/Aug. 1987.

[33] P. L. Jansen and R. D. Lorenz, "A physically insightful approach to the design and accuracy assessment of flux observers for field oriented induction machine drives," IEEE Trans. Ind. Applicat., vol. 30, pp. 101–110, Jan./Feb. 1994.

[34] G. C. Verghese and S. R. Sanders, "Observers for flux estimation in induction machines," IEEE Trans. Ind. Electron., vol. 35, pp. 85–94, Feb. 1988.

[35] H. Kubota, K. Matsuse, and T. Nakano, "DSP-based speed adaptive flux observer of induction motor," IEEE Trans. Ind. Applicat., vol. 29, pp. 344–348, Mar./Apr. 1993.

[36] Marko Hinkkanen and Jorma Luomi, "Parameter Sensitivity of Full-Order Flux Observers for Induction Motors," IEEE Transactions on Industry Applications, vol. 39, no. 4, pp. 1135-1127, July/August 2003.

[37] Y. A. Kwon and S. H. Kim, "A new scheme for speed-sensorless control of induction motor," IEEE Trans. Ind. Electron., vol. 51, no. 3, pp. 545–550, Jun. 2004.

[38] M. N. Uddin, and and Ronald S. Rebeiro, "Online Efficiency Optimization of a Fuzzy-Logic-Controller-Based IPMSM Drive," IEEE Transactions on Industry Applications, 2011, 47, (2), pp. 1043-1050.

[39] Casey B. Butt, M. Ashraful Hoque, and M. Azizur Rahman," Simplified Fuzzy-Logic-Based MTPA Speed Control of IPMSM Drive" IEEE Transactions on Industry Applications, Vol. 40, No. 6, pp. 1529-1535, November/December 2004.

[40] Jae-Sung Yu, Sang-Hoon Kim, Byoung-Kuk Lee, Chung-Yuen Won, and Jin Hur "Fuzzy-Logic-Based Vector Control Scheme for Permanent-Magnet Synchronous Motors in Elevator Drive Applications" IEEE Transactions on Industrial Electronics, Vol. 54, No. 4, pp. 2190-2200, August 2007.

[41] L. Harnefors, S. E. Saarakkala, and M. Hinkkanen, Speed Control of Electrical Drives Using Classical Control Methods, IEEE Transactions On Industry Applications, vol. 49, no. 2, pp. 889-898, 2013.

[42] Slobodan Vukosavic, "Digital Control of Electrical Drives," 2007 Springer.

[43] Mohamed S. Zaky, "A self-tuning PI controller for the speed control of electrical motor drives," Electric Power Systems Research, vol. 119, pp. 293–303, 2015.

Mohamed S. Zaky was born in Minoufiya, Egypt, on January 11, 1978. He awarded B.Sc. (with first-class honors), M.Sc., and Ph.D. degrees in Electrical Engineering from Minoufiya University, Shebin El-Kom, Egypt, in 2001, 2005, and 2008, respectively. In 2002, he became an instructor with Minoufiya University and then an assistant lecturer in 2006. In 2008–2013, he was a lecturer in the Department of Electrical Engineering, Faculty of Engineering; Minoufiya University. From 2013 to the present, Dr. Zaky has been an assistant professor with the Department of Electrical Engineering, Faculty of Engineering, Minoufiya University.

He has authored or coauthored over 37 papers. His research interests include control of electrical machines, applications of power electronics, DSP-based real-time control, sensorless control, and renewable energy applications.

Mohamed K. Metwaly was born in Minoufiya, Egypt, on January 20, 1974. He awarded B.Sc. (with first-class honors), M.Sc. degrees in Electrical Engineering from Minoufiya University, Shebin El-Kom, Egypt, in 1999, and 2003, respectively. In 2009, he awarded Ph.D. (with first-class honors) degree in electrical engineering from Vienna University of Technology, Vienna, Austria. . In 2000, he became an instructor with Minoufiya University and then an assistant lecturer in 2003. In 2010–2015, he was a lecturer in the Department of Electrical Engineering, Faculty of Engineering; Minoufiya University. From 2015 to the present, Dr. Metwaly has been an assistant professor with the Department of Electrical Engineering, Faculty of Engineering, Minoufiya University.

His research interests include ac machines control, power electronics, motor drives, the transient electrical behavior of ac machines, sensorless control techniques, and digital signals processing.